Electronic Supplementary Material (ESI) for Analyst.

Supporting Information

Silver nanoparticles aggregates on metal fiber for solid phase microextraction-surface enhanced Raman spectroscopy detection of polycyclic aromatic hydrocarbons

Cuicui Liu,[a] Xiaoli Zhang,[a] Limei Li,[b] Jingcheng Cui,[a] Yu-e Shi,[a] Le Wang[a] and Jinhua Zhan*,[a]

[a]National Engineering Research Center for Colloidal Materials and Key Laboratory of Colloid and Interface Chemistry, Ministry of Education, Department of Chemistry, Shandong University, Jinan 250100, China

[b]Department of Physics, Xiamen University, Xiamen Fujian, 361005, P. R. China

[c]Center of Technology, Jinan Entry-Exit Inspection and Quarantine Bureau, Jinan 250014, China

*Address for correspondence. Email: jhzhan@sdu.edu.cn
Phone: 86-531-88365017; Fax: 86-531-88366280

1. The SERS effect of oxidized AgNPs/Ag-Cu fiber.

2. Cyclic voltammetric of AgNPs/Ag-Cu fiber and PTH modified AgNPs/Ag-Cu fiber in 0.1 M KCl solution.

3. SEM image of commercial Ag-Cu fiber.

4. SEM images of the SERS-active fiber for sixteen cycles (A); twenty cycles (B); after modification with PTH (C); Cross-sectional SEM image of the SERS-active fiber (D).

5. The XPS spectra of the SERS-active fiber after modification with PTH.

6. The XPS spectra of quantitative Ag3d.

7. SERS and Raman spectra of the PTH.

8. SERS spectra of fluoranthene (1.00×10^{-5} M) on the SERS-active SPME fiber with different alkanethiol.

9. Simulated (FDTD) spatial of the electric field of crossed silver nanoparticles.

10. The length of the three alkanethiols, which were optimized using Gaussian 03 program (B3LYP, 6-31G).

11. The enhancement factor of different alkanethiol.

12. SERS spectra of fluoranthene (1.00×10^{-5} M) on the SERS-active SPME fiber with different cycles.

13. The stability of the SERS-active SPME fiber. SERS spectra of 1.00×10^{-5} M fluoranthene were recorded from fibers stored over a number of days under ambient conditions.

14. The uniformity of the SERS-active SPME fiber probed with 1.00×10^{-5} M fluoranthene without normalization.

15. The reproducibility of the SERS-active SPME fibers probed with 1.00×10^{-8} M fluoranthene.

16. Structures of PAHs in this work.

17. The SERS spectra of benzo(b)fluoranthene.

18. Selection of the internal standard peak.

19. The calculation of limit of detection.

20. The calculation of EF (Enhancement factor) of AgNPs/Ag-Cu fiber.

1. The SERS effect of oxidized AgNPs/Ag-Cu fiber.

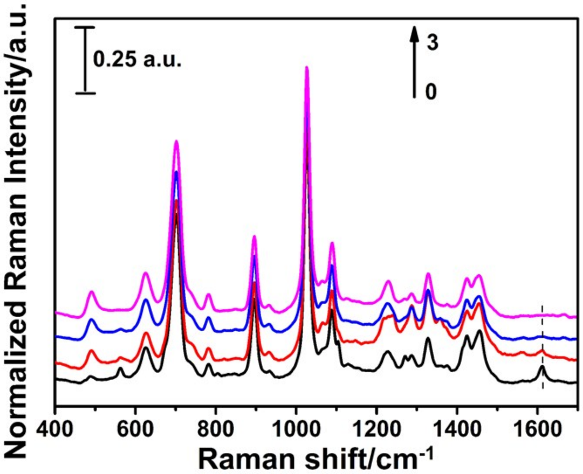

Figure S1. The SERS effect of oxidized AgNPs/Ag-Cu fiber. The AgNPs/Ag-Cu fibers were stored in air for several days, and then immersed in 1.00×10^{-3} M propanethiol for 12 h. The SERS-active SPME fibers were immersed in 1.00×10^{-5} M fluoranthene and their SERS spectra were recorded. The intensity decreases with the increase of oxidation time. The SERS signals of fluoranthene disappear, when the AgNPs/Ag-Cu fibers are stored in air for 3 days.

2. Cyclic voltammetric of AgNPs/Ag-Cu fiber and PTH modified AgNPs/Ag-Cu fiber in 0.1 M KCl solution.

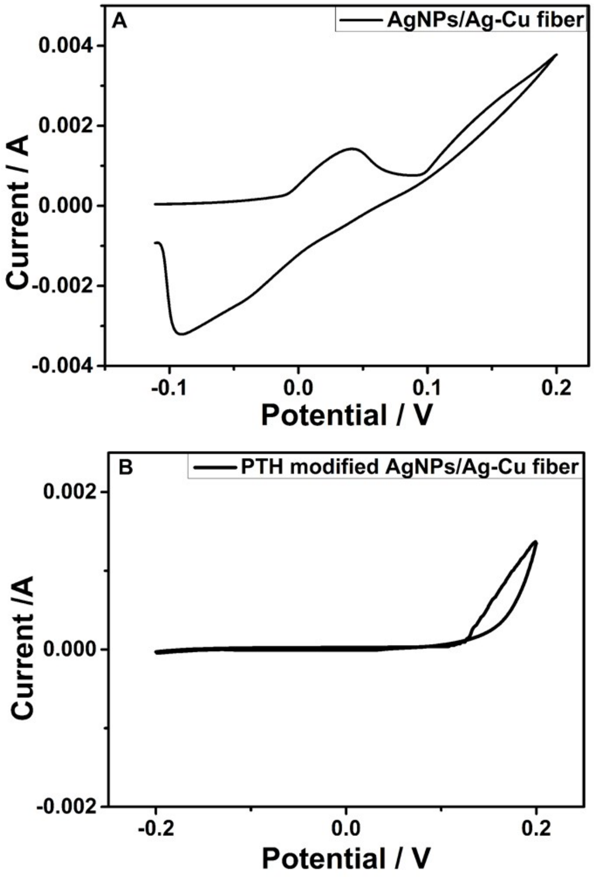

Figure S2. (A) Cyclic voltammetric of AgNPs/Ag-Cu fiber in 0.1 M KCl solution, (B) Cyclic voltammetric of PTH modified AgNPs/Ag-Cu fiber in 0.1 M KCl solution. The complete self-assembled monolayer over the entire surface of the nanoparticle was evaluated by cyclic voltammetric incorporating three electrodes: a working electrode, a reference electrode (Ag/AgCl) and an auxiliary electrode (Ti).[1-3]

3. SEM image of commercial Ag-Cu fiber.

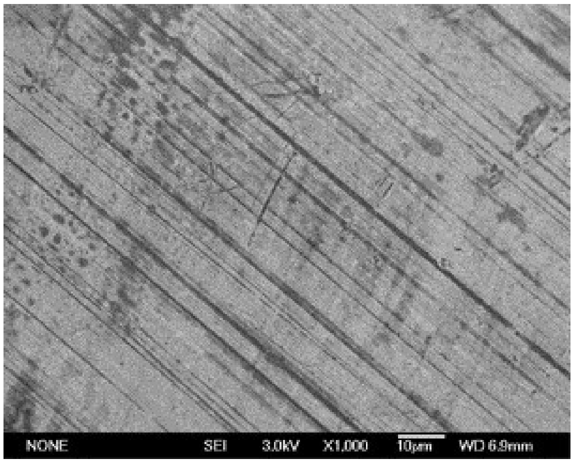

Figure S3. SEM image of commercial Ag-Cu fiber.

4. SEM images of the SERS-active fiber for sixteen cycles (A); twenty cycles (B); after modification with PTH (C); Cross-sectional SEM image of the SERS-active fiber (D).

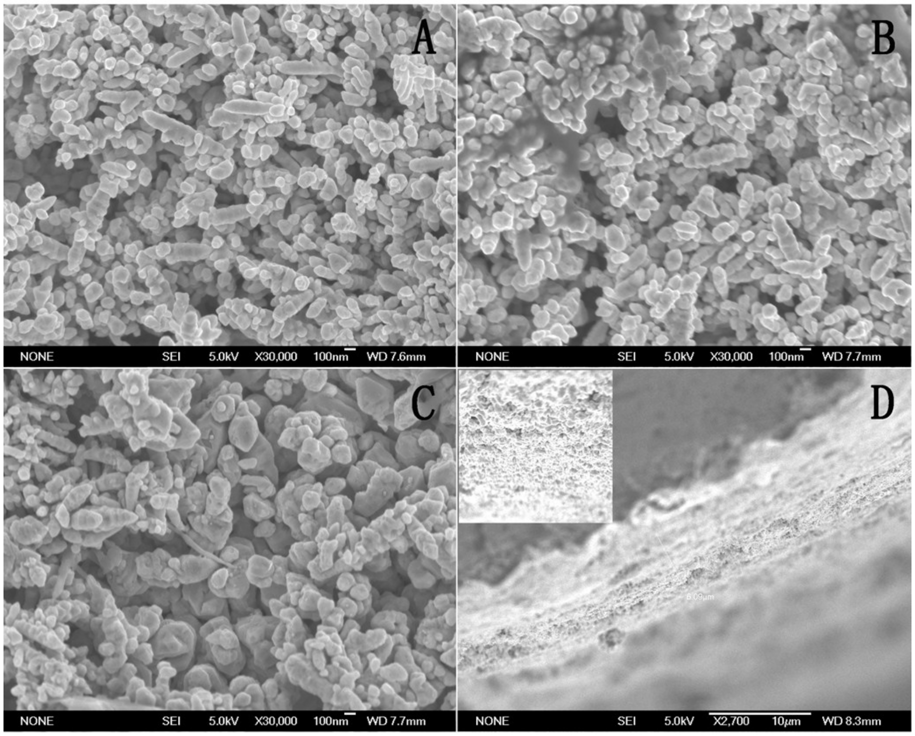

Figure S4. SEM image of silver nanoparticles on the silver-copper fiber with the assistant of Sn^{2+}, for sixteen cycles (A), for twenty cycles (B); (C) SEM image of the PTH modified AgNPs/Ag-Cu fiber with sixteen cycles; (D) Cross-sectional SEM image of the SERS-active fiber .

5. The XPS spectra of the SERS-active fiber after modification with PTH.

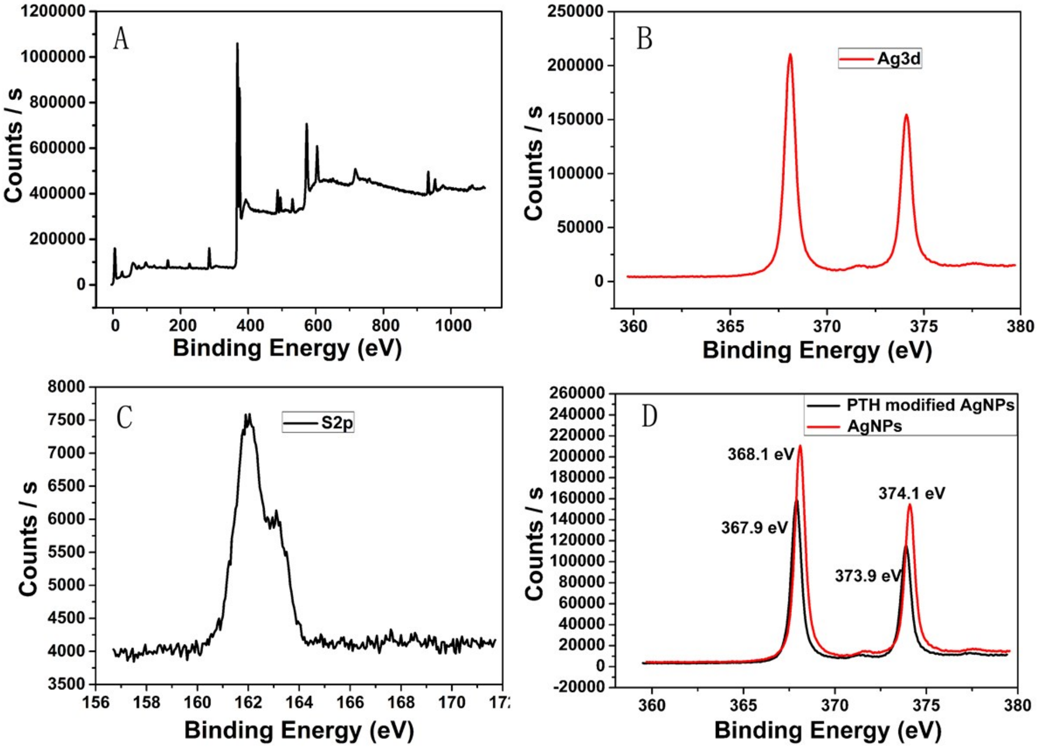

Figure S5. The XPS spectra of the SERS-active fiber after modification with PTH. (A) Survey scan for the PTH modified silver nanoparticles, immobilized on silver-copper fiber; Ag 3d (B), S 2p (C) regions of the XPS spectrum of the PTH modified silver nanoparticles, immobilized on silver-copper fiber and (D) XPS spectra for the SPME fiber before propanethiol self-assembled (red) and after propanethiol self-assembled (black). All of the reported spectra have been normalized to the same counts value. Silver binding energy shifted to lower value by 0.2 eV might be attributing to the formation of

Ag-S bond.

6. The XPS spectra of quantitative Ag3d.

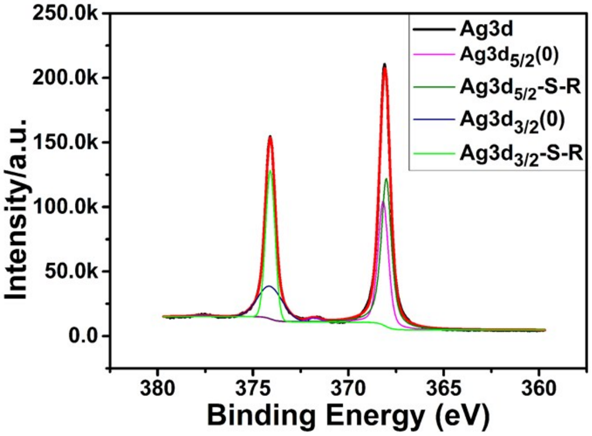

Figure S6. The XPS spectra of quantitative Ag3d.

7. SERS spectra of PTH (black line), Raman spectrum of liquid PTH served as a reference (red line).

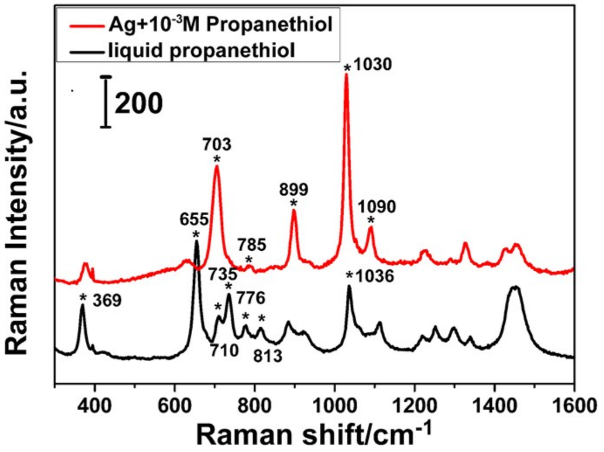

Figure S7. SERS spectra of PTH (black line), Raman spectrum of liquid PTH served as a reference (red line). Compared with the normal Raman spectrum of liquid propanethiol, both the number of Raman peaks and relative intensities had some differences.

Spectral data on the assignment of vibrational band of liquid propanethiol, SERS spectra of Ag-S$(CH_2)_2CH_3$, as shown in the following table.[4-6]

$CH_3(CH_2)_2SH$, (pure liquid)	Assignment	Ag-S$(CH_2)_2CH_3$, SERS(10^{-3}M),	Assignment
369s	CCC bend, gauche	703s	C-S stretch, trans
655vs	C-S stretch, gauche	785vw	CH_2 rock, gauche
710m	C-S stretch, trans	899w	CH_2 rock, gauche
735s	C-S stretch, gauche	1030m	C-C stretch, trans
776m	CH_2 rock, gauche	1090m	C-C stretch, gauche
813w	CSH deformation, trans		
1036vs	C-C stretch, trans		

Band frequencies are given in cm^{-1}; vibration intensities are denoted as vs(very strong), s(strong)，m(medium), w(weak), vw(very week); T and G represent rotational isomers of propanethiol in the trans and the gauche conformations with respect to the central C–C bond, respectively.

8. SERS spectra of fluoranthene on the SERS-active SPME fiber with different alkanethiol.

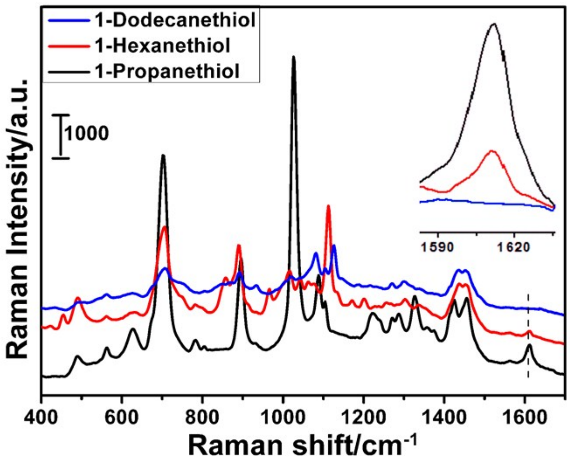

Figure S8. SERS spectra of fluoranthene (1.00×10^{-5} M) on the SERS-active SPME fiber with different alkanethiol.

9. Simulated (FDTD) spatial of the electric field of crossed silver nanoparticles.

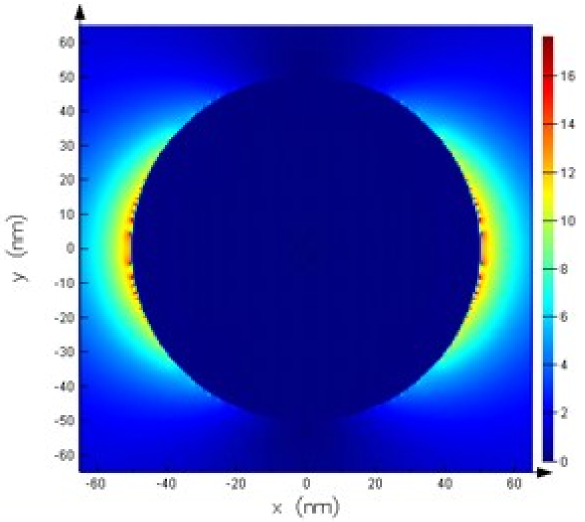

Figure S9. Simulated (FDTD) spatial of the electric field of crossed silver nanoparticles.

10. The length of the three alkanethiols, which were optimized using Gaussian 03 program (B3LYP, 6-31G).

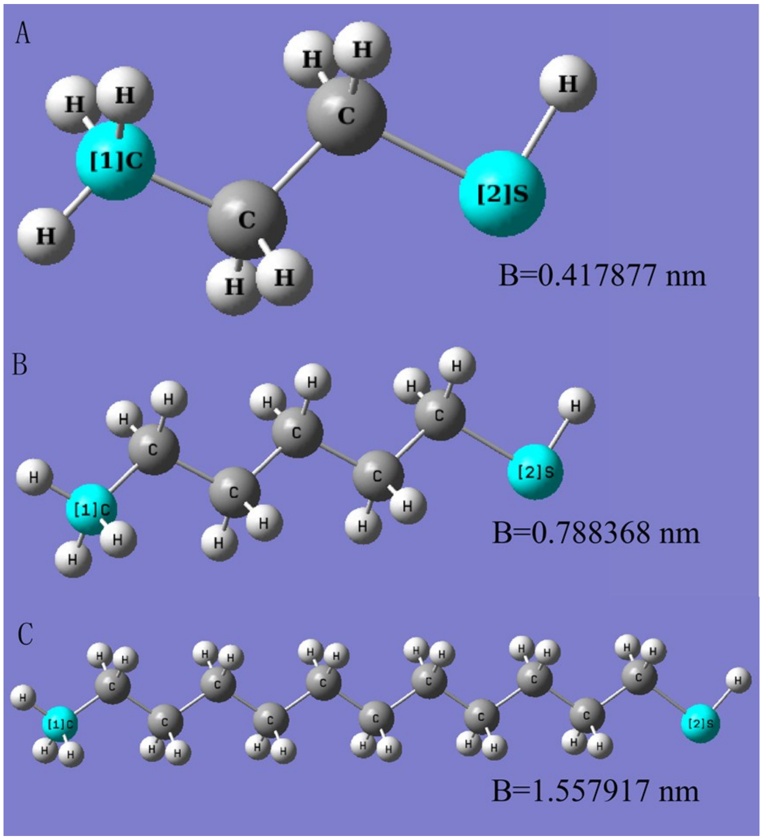

Figure S10. Structure optimization and length of alkanethiols.

11. The enhancement factor of different alkanethiol.

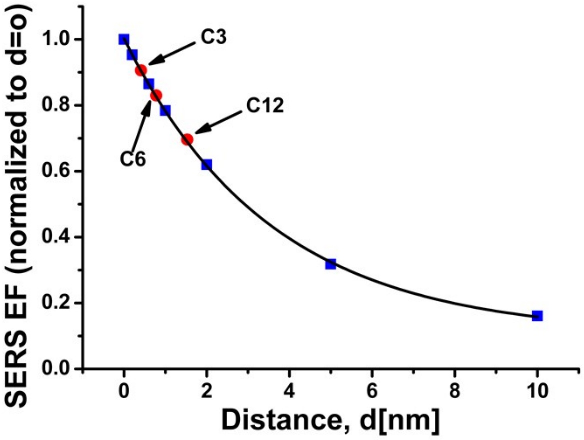

Figure S11. The enhancement factor of different alkanethiol, which was normalized d=0.

12. SERS spectra of fluoranthene (1.00×10^{-5} M) on the SERS-active SPME fiber with different cycles.

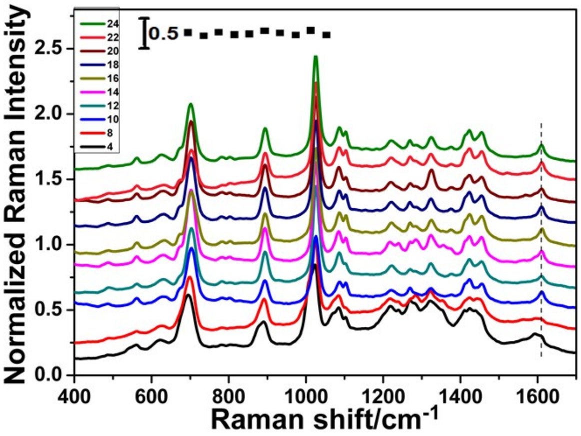

Figure S12. SERS spectra of fluoranthene (1.00×10^{-5} M) on the SERS-active SPME fiber with different cycles.

13. The stability of the SERS-active SPME fiber. SERS spectra of 1.00×10^{-5} M fluoranthene were recorded from fibers stored over a number of days under ambient conditions.

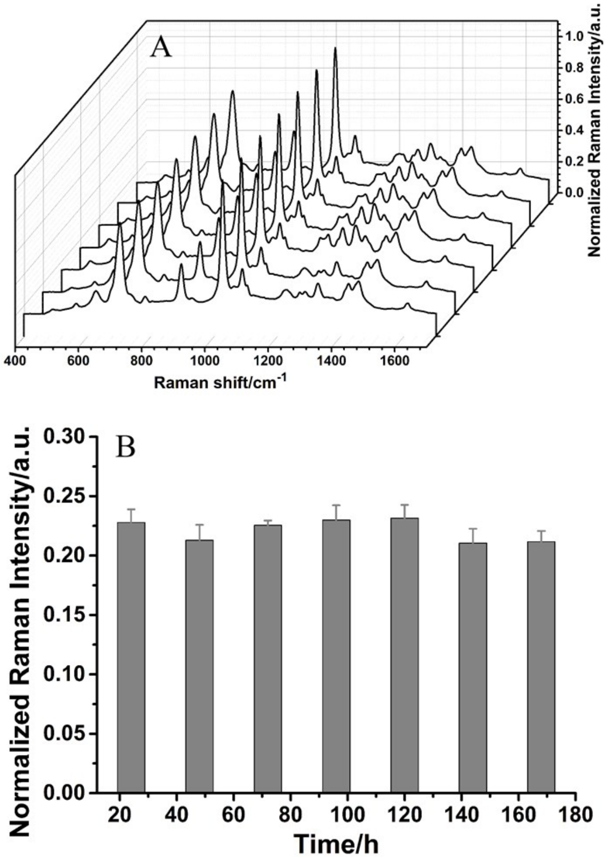

Figure S13. (A) Stability of the SERS-active SPME fiber. SERS spectra of 1.00×10^{-5} M fluoranthene were recorded from fibers stored over a number of days under ambient conditions, (B) The normalized Intensity at 1612 cm^{-1} over 7 days.

14. The uniformity of the SERS-active SPME fiber probed with 1.00×10^{-5} M fluoranthene without normalization.

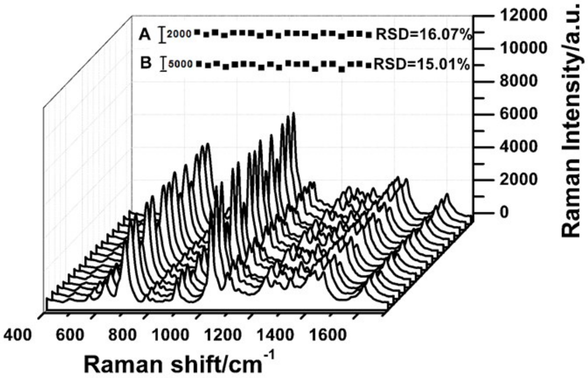

Figure S14. The uniformity of the SERS-active SPME fiber probed with 1.00× 10^{-5} M fluoranthene without normalization.

15. The reproducibility of the SERS-active SPME fibers probed with 1.00×10^{-8} M fluoranthene.

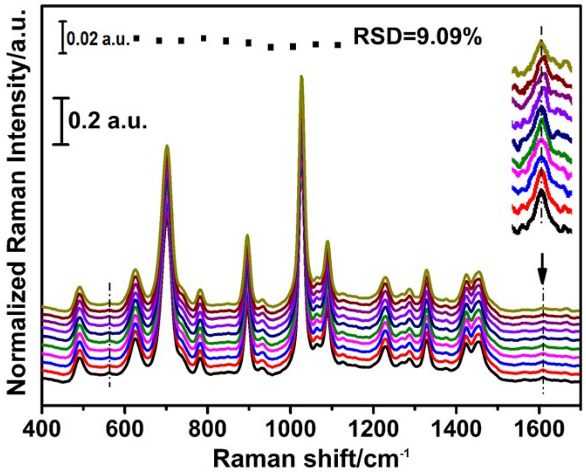

Figure S15. The reproducibility of the SERS-active SPME fibers probed with 1.00×10^{-8} M fluoranthene.

16. Structures of PAHs in this work.

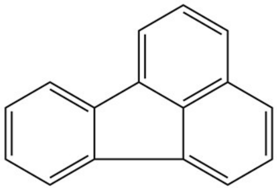

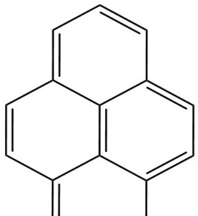

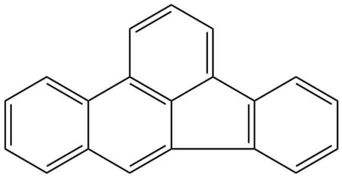

Fluoranthene Pyrene Benzo(b)fluoranthene

Figure 16. Structures of PAHs in this work

17. The SERS spectra of benzo(b)fluoranthene

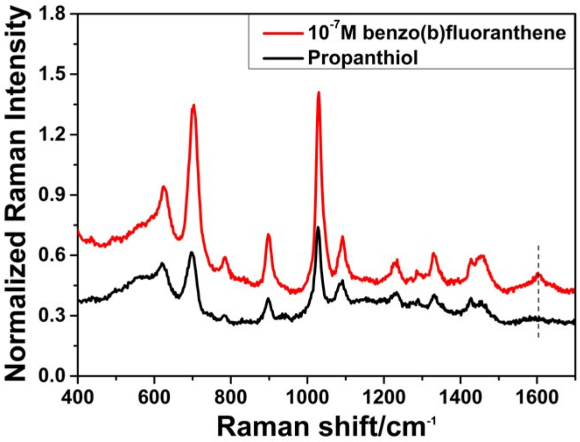

Figure S17. The SERS spectra of benzo(b)fluoranthene

18. Selection of the internal standard peak.

Raman peak position	$1030\ cm^{-1}$	$1090\ cm^{-1}$
Vibrational mode	$\nu(C\text{-}C)_T$	$\nu(C\text{-}C)_G$
RSD	5.66%	7.51%

Table S1. Comparison of the relative standard deviation (RSD) with different internal standard. T and G represent rotational isomers of propanethiol in the trans and the gauche conformations with respect to the central C-C bond, respectively.[2]

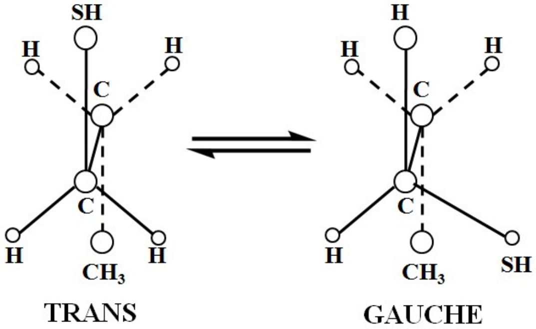

19. The calculation of limit of detection (LOD).

LOD was determined as three times the standard deviation.

y=three times the standard deviation.

x= the limit of detection.

	standard deviation	liner equation	detection limit
fluoranthene	0.00209	Logarithm y=-1.54622+0.20912 logarithm x	7.56×10^{-10}

Table S2. The LOD of fluoranthene.

20. The calculation of EF (Enhancement factor) of AgNPs/Ag-Cu fiber.

The SERS enhancement factor for p-aminothiophenol was calculated by the following equation:

$EF= (I_{SERS}/I_{Raman}) \cdot (N_{bulk}/N_{ads})$

$N_{ads} = A/A_{sum} \cdot V_{ads} \cdot C_1$

$N_{bulk} = A \cdot H_{eff} \cdot C_{sol}$

N_{ads} is the number of p-aminothiophenol molecules under laser radiation adsorbed on substrate;

A_{eff} is the effective area of spot size;

A_{sum} is the area of the fiber substrate, id=0.35mm, length=1cm;

V_{ads} is the volume that is spotted onto the paper substrate, 10 μL;

C_1 is the concentration of the solution that is to be measured.

N_{bulk} is the number of p-aminothiophenol molecules in the scattering volume in bulk solution;

H_{eff} is the effective length of of the scattering volume and here was estimated as the depth of field, 2.2 mm;

C_{sol} is 0.1 M p-aminothiophenol power for the non-SERS measurement.

$$
\begin{aligned}
EF(\text{fluoranthene}) &= (I_{SERS}/I_{Raman}) \cdot (A_{eff} \cdot H_{eff} \cdot C_{sol}) / (A_{eff}/A_{sum} \cdot V_{sum} \cdot C_1) \\
&= (I_{SERS}/I_{Raman}) \cdot (A_{sum} \cdot H_{eff} \cdot C_{sol}) / (V_{ads} \cdot C_1) \\
&= 0.0024178 \cdot (I_{SERS} \cdot C_{sol}) / (I_{Raman} \cdot C_1) \\
&= 1.59 \times 10^5
\end{aligned}
$$

References

1. K. Bandyopadhyay, M. Sastry, V. Paul, K. Vijayamohanan, *Langmuir* **1997**, 13, 866-869.

2. M. French, S. E. Creager, *Langmuir* **1998,** 14, 2129-2133.

3. J. D Zhang, Q. J. Chi, J. Ulstrup, *Langmuir* **2006**, 22, 6203-6213

4. R. E. Pennington, D. W. Scott, H. L. Finke, J. P. McCullough, J. F. Messerly, I. A. Hossenlopp, G. Waddington, *J. Am. Chem. Soc.* **1956**, 78, 3266-3272.

5. A. Kudelski, *J. Raman Spectrosc.* **2003**, 34, 853-862.

6. N. D. Strekal, A. E. German, G. A. Gachko, S. A. Maskevich, *Optics and Spectroscopy* **2000**, 89, 834-840.